

# Investigation of an anisotropic tortuosity in a Biot model of ultrasonic propagation in cancellous bone

Elinor R. Hughes, Timothy G. Leighton,<sup>a)</sup> and Paul R. White

*Institute of Sound and Vibration Research, University of Southampton, Southampton, SO17 1BJ, United Kingdom*

Graham W. Petley

*Department of Medical Physics and Bioengineering, Southampton University Hospitals NHS Trust, Tremona Road, Southampton, SO16 6YD, United Kingdom*

(Received 10 June 2006; revised 12 October 2006; accepted 12 October 2006)

The modeling of ultrasonic propagation in cancellous bone is relevant to the study of clinical bone assessment. Historical experiments revealed the importance of both the viscous effects of bone marrow and the anisotropy of the porous microstructure. Of those propagation models previously applied to cancellous bone, Biot's theory incorporates viscosity, but has only been applied in isotropic form, while Schoenberg's anisotropic model does not include viscosity. In this paper we present an approach that incorporates the merits of both models, by utilizing the tortuosity, a key parameter describing pore architecture. An angle-dependent tortuosity for a layered structure is used in Biot's theory to generate the "Stratified Biot Model" for cancellous bone, which is compared with published bone data. While the Stratified Biot model was inferior to Schoenberg's model for slow wave velocity prediction, the proposed model improved agreement fast wave velocity at high propagation angles, particularly when sorted for porosity. An attempt was made to improve the fast wave agreement at low angles by introducing an angle-dependent Young's Modulus, which, while improving the agreement of predicted fast wave velocity at low angles, degraded agreement at high angles. In this paper the utility of the tortuosity in characterizing the architecture of cancellous bone is highlighted. © 2007 Acoustical Society of America. [DOI: 10.1121/1.2387132]

PACS number(s): 43.80.Cs, 43.80.Qf, 43.20.Jr [CCC]

Pages: 568–574

## I. INTRODUCTION

The skeleton contains two types of calcified tissue: cortical and cancellous. Cortical bone is dense and compact, while cancellous bone is a porous network of calcified "trabeculae," filled with fatty bone marrow (Fig. 1). There is much variety in the trabecular arrangement throughout the skeleton, and hence in the mechanical properties of cancellous bone, which may be isotropic at some sites (e.g., femoral head), or highly anisotropic at others (vertebrae, femur).<sup>1</sup>

Osteoporosis is a skeletal disease that reduces bone density and erodes the trabecular microstructure, leading to increased bone fragility. While a reduction in density can be assessed by Dual X-Ray Absorptiometry,<sup>2</sup> microstructure may potentially be examined using ultrasonic techniques. Quantitative Ultrasound<sup>2</sup> (QUS) analyses information from ultrasonic signals traveling through a skeletal site, often a site containing cancellous bone, such as the calcaneus. However, QUS parameters are not firmly linked to physical parameters, such as bone strength or porosity, other than through statistical means. Current research aims to establish such relations through a validated predictive propagation model. Biot's theory, and Schoenberg's theory for propagation in porous media, have both been applied to the problem.

Biot's theory<sup>3</sup> of wave propagation in a porous solid saturated with fluid, predicts two compressional waves (fast

and slow waves) and a shear wave. The theory was first applied to ultrasonic propagation in cancellous bone in 1991 by McKelvie and Palmer,<sup>4</sup> and has since been used by several authors, with varying degrees of success.<sup>5–12</sup> Two compressional waves in cancellous bone at ultrasonic frequencies were first observed by Hosokawa and Otani,<sup>8</sup> and later confirmed by the present authors.<sup>9</sup> Further workers have applied modified Biot models to the problem.<sup>10,11</sup> One disadvantage of Biot's theory is that it requires knowledge of over a dozen input parameters, many of which are not easily evaluated for biological tissue.

The present authors used Schoenberg's theory<sup>9</sup> to predict the well-documented anisotropic behavior of ultrasonic properties in cancellous bone.<sup>13–15</sup> By imagining the microstructure of highly oriented cancellous bone as an array of bone-marrow layers, the use of Schoenberg's theory for a stratified composite medium provided the first anisotropic model, giving qualitative agreement with measured fast and slow wave phase velocities. One disadvantage of the Schoenberg model lies in its simplicity; for example, it takes no account of fluid viscosity. Replacing interstitial marrow by another fluid, such as water, is known to affect wave properties in cancellous samples,<sup>16</sup> owing to a difference in viscosity ( $\eta_{\text{marrow}}=0.15$  Pa s;  $\eta_{\text{water}}=0.0001$  Pa s, at 20 °C). Therefore any propagation model for bone should also account for this factor.

In this paper we present a simple approach that incorporates the merits of both Biot's theory and Schoenberg's

<sup>a)</sup>Electronic mail: T.G.Leighton@soton.ac.uk

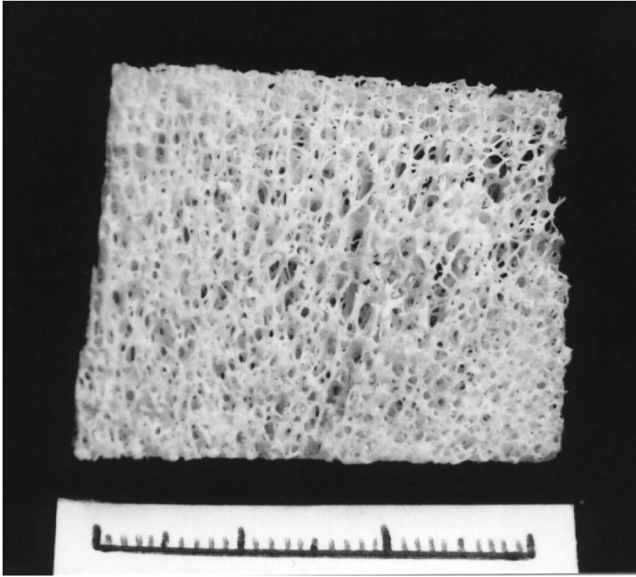


FIG. 1. The porous microstructure of cancellous bone from a bovine femur, showing a centimeter scale.

theory. This is done by introducing anisotropy into Biot's theory through an angle-dependent tortuosity for layers, to create a "stratified Biot" model. The performance of the models is compared with each other and with experimental data. Analysis is limited to the consideration of phase velocity, owing to complex problems in the comparison of predicted absorption with measured signal loss.<sup>9</sup>

## II. BIOT'S THEORY

Biot's theory<sup>3</sup> considers acoustic wave propagation in an isotropic porous elastic solid (of density,  $\rho_s$ ; moduli,  $E_s$ ,  $K_s$ , and  $N$ ; porosity,  $\beta$ ), saturated with a viscous fluid (of density,  $\rho_f$ ; moduli,  $E_f$  and  $K_f$ ; and viscosity  $\eta$ ). The theory is valid for frequencies where the wavelength is large relative to the size of the discontinuities. For a harmonic pressure wave, phase velocity and attenuation are found from

$$V_{\text{fast,slow}} = \sqrt{\frac{\Delta \pm [\Delta^2 - 4(PR - Q^2)(\rho_{11}\rho_{22} - \rho_{12}^2)]^{1/2}}{2(\rho_{11}\rho_{22} - \rho_{12}^2)}}, \quad (1)$$

$$V_{\text{shear}} = \sqrt{N/[(1 - \beta)\rho_s + (1 - 1/\alpha)\rho_f]}, \quad (2)$$

where  $\Delta = P\rho_{22} + R\rho_{11} - 2Q\rho_{12}$ . The terms  $A$ ,  $Q$ ,  $P$ , and  $R$  are generalized elastic coefficients that are defined in terms of the bulk moduli of the solid frame,  $K_b$ , the solid material,  $K_s$ , and the fluid,  $K_f$ , which can be found from standard expressions for an isotropic medium. The mass density terms,  $\rho_{ij}$ , are defined in terms of porosity and density, as given in the literature.<sup>3</sup> Equation (1) governs the propagation of two compressional waves, known as fast and slow waves, and Eq. (2) describes shear wave propagation. The fast wave is a bulk wave where the fluid and solid are locked together through viscous or inertial coupling, where as the slow wave corresponds to there being a relative motion between the fluid and the solid.

Below a specific "critical frequency" viscous coupling dominates, allowing fast wave propagation, but impeding the slow wave, which becomes diffusive. Above the critical frequency, viscous coupling weakens and inertial coupling dominates. In cancellous bone *in vitro*, the critical frequency is typically below<sup>17</sup> 1 kHz, hence at ultrasonic frequencies of interest, inertial coupling dominates.

The extent of inertial coupling,  $\rho_{12}$ , depends on the geometry of the porous solid, as described by

$$\rho_{12} = -(\alpha - 1)\beta\rho_f, \quad (3)$$

where  $\alpha$  is the tortuosity, a crucial parameter in Biot's theory. It represents the squared ratio of the mean pathlength through the porous frame to that of the direct path. In a nonviscous fluid, the tortuosity is real-valued, being between 1 (for  $\beta=1$ ), and tending to infinity, as  $\beta \rightarrow 0$ . It may be defined for a specific porous geometry, noted here as  $\alpha_\infty$ . For example, for a geometry of fused spheres,<sup>18</sup> the tortuosity,  $\alpha_\infty$ , is

$$\alpha_\infty = 1 - s \left( 1 - \frac{1}{\beta} \right), \quad (4)$$

where the structure factor,  $s=1/2$ . Also, for a medium of cylindrical tubes,<sup>19</sup> at a propagation angle  $\theta$  to the pores, the tortuosity is

$$\alpha_{\text{tubes}} = 1/\cos^2 \theta, \quad (5)$$

which equals unity for propagation along the pores.

The importance of  $\alpha_\infty$  is apparent when considering propagation in porous media having a rigid frame ( $K_b \gg K_f$ ,  $K_s \gg N$ ), where the velocity of the slow wave is<sup>20</sup>  $V_{\text{slow}} = V_{\text{fluid}}/\sqrt{\alpha_\infty}$ .

Equation (3) may be written to account for frequency-dependent effects, as

$$\rho_{12}(\omega) = -[\alpha(\omega) - 1]\beta\rho_f, \quad (6)$$

where  $\alpha(\omega)$  is the dynamic tortuosity. Johnson *et al.*<sup>20</sup> defined  $\alpha(\omega)$  in terms of measurable parameters as

$$\alpha(\omega) = \alpha_\infty + j\eta\beta \left( 1 - \frac{4j\alpha_\infty^2 k_0^2 \rho_f \omega}{\beta^2 a^2} \right) / \omega\rho_f k_0, \quad (7)$$

where  $a$  is a pore size parameter (often the pore radius), and  $k_0$  is the permeability for static conditions.

The geometric tortuosity  $\alpha_\infty$  in Eq. (7) can be evaluated by different methods. First, the "electrical conductivity" method involves measuring the ratio of the conductivity of saline alone to a sample saturated with saline,  $F$ , and using the relationship  $\alpha_\infty = F\beta$ . Tortuosity may also be measured using the nonviscous superfluid <sup>4</sup>He in the pores<sup>20</sup> or by a slow wave method, involving relation  $V_{\text{slow}} = V_{\text{fluid}}/\sqrt{\alpha_\infty}$  for rigid frame media. The reflection and transmission of pulses of ultrasonic<sup>21</sup> and audio<sup>22</sup> frequencies have also been used to deduce the tortuosity and porosity of air-filled rigid frame media.

## III. TORTUOSITY IN CANCELLOUS BONE

The tortuosity of cancellous bone has been defined and evaluated in different ways. Table I summarizes some results

TABLE I. Input parameters for the stratified Biot and Schoenberg models.

Authors	Bone type	Exp. Tortuosity	Method
Williams <i>et al.</i> , 1996	Human calcaneus	1.6 for $a=0.5$ mm	Electrical conductivity
Lauriks <i>et al.</i> , 1994	Bovine	1.26 to 2.64 (various porosities)	Electrical conductivity
Strelitzki <i>et al.</i> , 1999	Human calcaneus	1.04	Transmitted slow wave, at 400 kHz
Fellah <i>et al.</i> , 2004	Human femur	1.02 to 1.05	Reflected slow wave method at 2.25 MHz
Attenborough <i>et al.</i> , 2005	Phantoms of femoral head calcaneus	1.3 to 1.8 1.1 to 1.7	Reflected slow wave method at 1 kHz

of tortuosity in cancellous bone, with values varying between 1.01 and 2.6. Initial consideration of Table I suggests that ‘slow wave’ methods at ultrasonic frequencies yield lower results when compared with data taken at audio frequencies or by the electrical conductivity method. This may be because ultrasonic tests are more likely to be affected by scattering. Although the data in Table I does not allow skeletal sites to be classified by tortuosity, Attenborough *et al.*<sup>22</sup> recently demonstrated that average tortuosity differs between sites, with highly oriented microstructures (lumbar spine) yielding tortuosities closer to unity than those less oriented sites (e.g., femoral head). More significantly, tortuosity was orthogonally anisotropic.

In propagation models, some workers<sup>5,8,12</sup> used the purely geometric definition of Eq. (4), while others applied the dynamic tortuosity of Eq. (7).<sup>6,7,9,11</sup> In Biot simulations, Fellah *et al.*<sup>11</sup> demonstrated that a 20% increase in tortuosity produced a 10% decrease in wave velocities, a 300% increase in the fast wave amplitude, and a 60% decrease in the slow wave amplitude, highlighting the sensitivity of wave properties to this factor.

Using the tortuosity to characterize the cancellous structure has significant potential, since it may be able to describe architecture with a greater value and significance than parameters such as porosity or pore size. Recognizing the angular dependence of the tortuosity, with respect to trabecular orientation, is the subject of the remainder of this paper, after a discussion of Schoenberg’s plate model.<sup>23</sup>

#### IV. SCHOENBERG’S THEORY FOR STRATIFIED MEDIA

In Schoenberg’s theory,<sup>24</sup> for propagation in periodically alternating fluid-solid layers, strata are parallel to  $x$  and  $y$  directions, with spatial period,  $H$ , in the  $z$  direction (Fig. 2) and porosity,  $\beta$ . The solid is isotropic and elastic, with density  $\rho_s$ , compressional speed  $V_s$ , and shear speed,  $V_{sh}$ , while the fluid is ideal, nonviscous, with sound speed  $V_f$ .

Wave propagation is expressed in terms of the slowness vector,  $\mathbf{s}=(s_x, s_y, s_z)$  and the components parallel to the layers,  $s_x$ , and normal to the layers,  $s_z$ , ( $x$  and  $y$  are interchangeable) are related by

$$(s_z^2/\langle\rho\rangle) - \left( \frac{\beta(V_f^2 - s_x^2)}{\rho_f} + \frac{(1-\beta)(V_s^2 - s_x^2)}{\rho_s(1 - V_{pl}^2 s_x^2)} \right) = 0, \quad (8)$$

where  $\langle\rho\rangle = \beta\rho_f + (1-\beta)\rho_s$ , and  $V_{pl}$  represents the plate speed in the solid

$$V_{pl} = 2 \left( 1 - \frac{V_{sh}^2}{V_s^2} \right)^{1/2} V_{sh}. \quad (9)$$

Phase velocity is the inverse of the magnitude of the slowness vector,  $|\mathbf{s}|^{-1}$ , at an angle  $\theta = \tan^{-1}(s_z/s_x)$ , where  $0^\circ$  is normal to the layers, and  $90^\circ$  is parallel to the layers. Schoenberg’s theory predicts two compressional waves equivalent to the fast and slow waves of Biot’s theory. Their phase velocities vary with propagation angle, owing to an anisotropic inertial coupling, which tends to infinity at  $0^\circ$  (normal to the layers where  $\alpha_\infty \rightarrow \infty$ ), varying to zero at  $90^\circ$  (parallel to the layers where  $\alpha_\infty = 1$ ).

In *in vitro* studies, Schoenberg’s theory gave qualitative agreement with measured data in bovine cancellous bone<sup>9</sup> and further success was reported by other authors<sup>25–27</sup> for various bone types.

While Schoenberg offers insight into the role of inertial coupling in layers, the theory clearly oversimplifies the cancellous structure. In addition, the omission of fluid viscosity in Schoenberg’s model prevents it from accounting for viscous absorption and restricts its application to Biot’s ‘‘high’’ frequency region. Biot’s theory, while accounting for viscous effects, has only been applied to cancellous bone in isotropic form. In the following section we develop a model that incorporates viscous effects and anisotropic effects into a Biot model in a simple and straightforward manner.

#### V. AN ANISOTROPIC BIOT MODEL FOR CANCELLOUS BONE

The angular variation in wave properties with respect to trabecular direction originates from two characteristics of

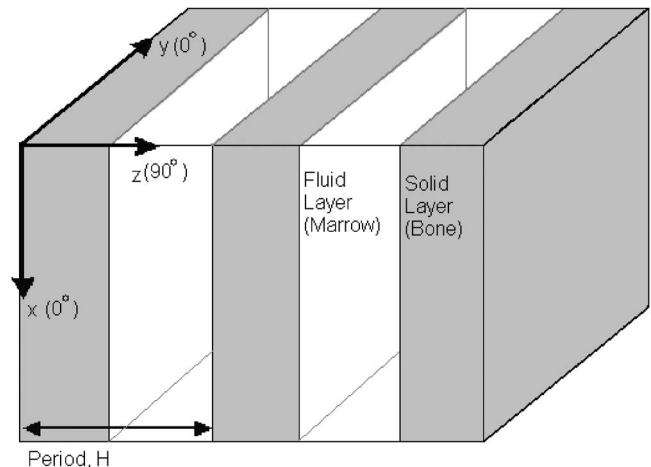


FIG. 2. Idealization of the structure of cancellous bone as an array of parallel bone-marrow layers.

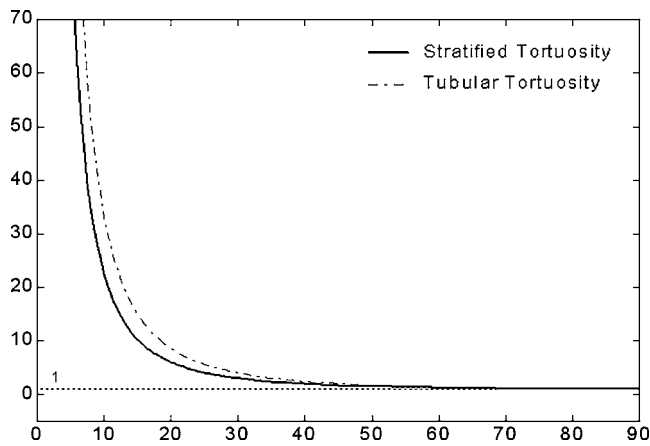


FIG. 3. Predicted stratified tortuosity of Eq. (20) (solid line), and tubular tortuosity,  $\alpha_{\text{tubes}}=1/\cos^2\theta$  (dashed line), versus the angle of propagation. The angle  $0^\circ$  is normal to the stratification.

cancellous bone: the mechanical properties of the bone matrix and the motion of the fluid within irregularly shaped pores. Previous models of propagation in anisotropic porous media have either been extremely generalized<sup>28</sup> and therefore complex, or specific to particular conditions of structure, frequency or constituent media.<sup>29</sup> The current approach introduces a pragmatic way of modeling an anisotropic stratified structure within the confines of a Biot model. This is done by using an angle-dependent tortuosity defined for layers of periodic bone-marrow plates, and inserting this back into Biot's theory. This approach was named the "Stratified Biot model," following the work of Schoenberg and Sen.<sup>30</sup>

The dependence of velocity on the direction in a stratified model reflects the variation in inertial coupling. The degree of inertial coupling within Schoenberg's layers may be assumed to be equivalent to that occurring in an arbitrary anisotropic porous medium as described by Biot's theory. Therefore, describing a layered structure in Biot's theory requires finding an expression for the tortuosity for a simple stratified structure as a function of the angle of propagation. Such an expression may be obtained by equating the compressional phase velocity in terms of  $\alpha$  from Biot's theory [Eqs. (1)], with that from Schoenberg's model in terms of propagation angle,  $\theta$  [Eqs. (8) and (9)]. In the first instance, this calculation may be substantially simplified if shear in the solid is neglected ( $K_b=N=0$  and  $PR-Q^2=0$ ). While effectively yielding a fluid-fluid system, this is a fruitful starting point in developing a tortuosity for a stratified medium. The tortuosity as a function of propagation angle,  $\alpha_{\text{layers}}(\theta)$ , can then be found as

$$\alpha(\theta) = 1 + [(1 - \beta)\rho_s/\langle\rho\rangle]\cot^2\theta. \quad (10)$$

Equation (10) may then be inserted back into Biot's theory, substituting for  $\alpha_\infty$ , to predict wave properties that vary with orientation. This approach will be known for the remainder of this paper as the "Stratified Biot" model.

Figure 3 shows the stratified tortuosity of Eq. (10) plotted as a function of angle, using values from Table II. The angle  $\theta=0^\circ$  is normal to the layers and  $\theta=90^\circ$  is parallel to the layers. For comparison, the tortuosity for an array of cylinders from Eq. (5) is plotted, with angle convention dic-

TABLE II. Input parameters for the stratified Biot and Schoenberg models.

Parameter	Value	Source
Density of Solid Bone, $\rho_s$	1960 kg/m <sup>3</sup>	Williams, 1992
Density of Marrow, $\rho_f$	990 kg/m <sup>3</sup>	Duck, 1990
Young's Modulus of Bone, $E_s$	20 GPa	Williams, 1992
Bulk Modulus of Marrow, $K_f$	2.2 GPa	Hosokawa and Otani, 1997
Poisson's ratio of solid, $\nu_s$	0.32	Williams, 1992; Duck 1990
Poisson's ratio of frame, $\nu_b$	0.32	Williams, 1992
Porosity, $\beta$	0.65–0.82	By experiment
Power index, $n$	1.23	Williams, 1992
Viscosity of marrow, $\eta$	0.04 Pa s	Bryant <i>et al.</i> , 1989
Pore radius, $a$	$5 \times 10^{-3}$ m	By experiment
Permeability, $k_0$	$5 \times 10^{-9}$ m <sup>3</sup>	McKelvie and Palmer, 1991
Frequency, $f$	1 MHz	By experiment
Solid compressional speed, $V_s$	3200 m/s	Williams, 1992
Fluid compressional speed, $V_f$	1500 m/s	Estimate
Shear speed, $V_{sh}$	1800 m/s	Wu and Cubberly, 1997 (Ref. 32)

tating correspondence between the dominant axes of both oriented systems (i.e.,  $\theta=0^\circ$  being normal to layers and tubes, Fig. 3). Figure 3 shows that both stratified and tubular tortuosities tend to infinity as  $\theta \rightarrow 0^\circ$ , and to unity as  $\theta \rightarrow 90^\circ$ . The two curves show a marked similarity in shape, however, the stratified tortuosity is a function of porosity, which thus provides added power to model changes in structure over Eq. (5).

## VI. RESULTS FOR CANCELLOUS BONE

Figure 4 shows the predictions of fast and slow wave velocities versus angle with respect to the structural orientation for the Stratified Biot model and Schoenberg's theory. The input parameters are listed in Table II. Stratified Biot fast and slow wave phase velocities were found from Eq. (1), using Eq. (10). Schoenberg's velocities were predicted as a function of the propagation angle, using Eqs. (8) and (9). The angle  $0^\circ$  is normal to the layers and  $90^\circ$  is parallel to the layers.

Each model predicts a pair of velocity contours that vary with angle. The fast wave corresponds to the upper curve of

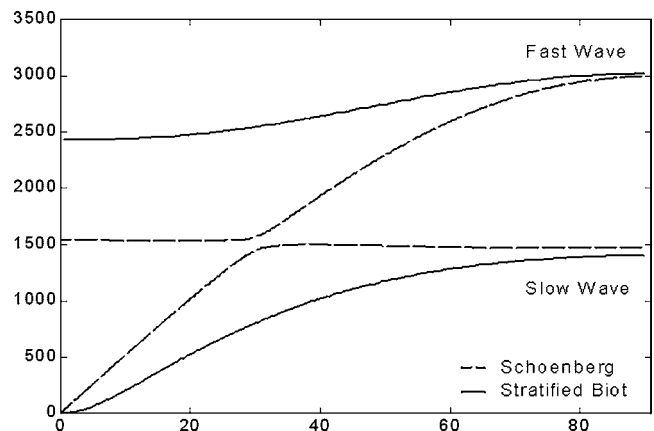


FIG. 4. Predicted fast and slow wave phase velocities for the stratified Biot model (solid line) and the Schoenberg model (dashed line). Angles  $0^\circ$  and  $90^\circ$  are normal and parallel to the stratification, respectively.

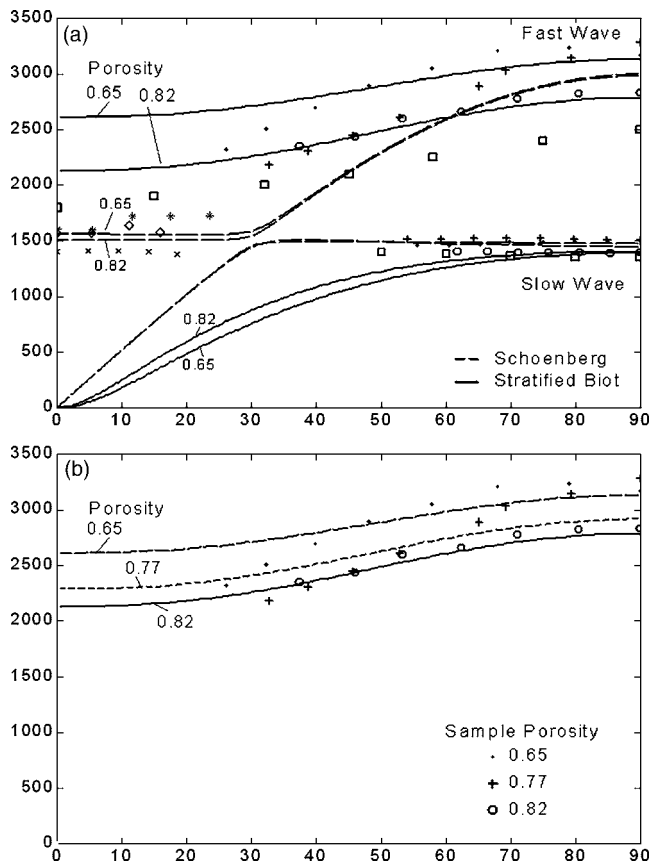


FIG. 5. (a) Predicted fast and slow wave velocities versus the angle of propagation for the stratified Biot model (solid lines) and the Schoenberg model (dashed lines). The angle  $0^\circ$  is normal to layering. Models are evaluated at porosities of 0.82 and 0.65, corresponding to the range within samples. Data from Hughes *et al.* (Ref. 6) ( $\cdot$ ,  $\circ$ ,  $+$ ,  $*$ ,  $x$ ,  $\diamond$ ), and Hosokawa and Otani (Ref. 16) ( $\square$ ). (b) Predicted fast wave velocities versus angle of propagation for the Stratified Biot model for input porosities of 0.65, 0.77, and 0.82 [data from Hughes *et al.* (Ref. 6)].

the pair, while the slow wave corresponds to the lower of the pair. Predictions from Schoenberg's theory (dashed lines) show a characteristic piecewise linear shape over most of the angular range, with the fast wave curve becoming nonlinear above  $60^\circ$ . By contrast, predictions from the stratified Biot model (solid lines) vary less sharply, converging with Schoenberg velocities at  $0^\circ$  and  $90^\circ$  for the slow wave, and  $90^\circ$  for the fast wave. A significant discrepancy between the models is seen in the fast wave, disagreeing by almost 50% at  $0^\circ$ . It should be noted that a degree of disagreement between the two approaches is to be expected, because the inclusion of anisotropy and viscosity in the stratified Biot model, for interpenetrating fluid and solid phases, will not make it identical to the Schoenberg model, for infinitely extending uninterrupted plates. Perhaps a better test of performance is to compare it with experiment.

In Figs. 5(a) and 5(b), previously published data from ultrasonic measurements of bovine femur<sup>9,15</sup> are compared with the predictions of Schoenberg (dashed lines) and the Stratified Biot model (solid lines). Full details of the experimental methods may be found in work by Hughes *et al.*<sup>9</sup> and Hosokawa and Otani.<sup>15</sup> Data from Hughes *et al.* was taken from six marrow-filled bovine femur samples of porosity between  $\beta=0.65$  and 0.82, and subject to errors in the measure-

ment of thickness, transducer separation, and insonation angle. The intersample precision was 6.0%. The porosity of the bovine femur sample tested by Hosokawa and Otani was  $\beta=0.82$ .

Figures 5(a) and 5(b) demonstrate the reproducible result that measured fast and slow wave phase velocities depend on the angle of propagation within cancellous samples. The fast wave velocity increases with angle, from around 2000–2200 m/s at  $30^\circ$  to between 2800–3200 m/s at  $90^\circ$  in Hughes' data, and from 1800 m/s at  $0^\circ$  to 2500 m/s at  $90^\circ$  in the data of Hosokawa and Otani data. By contrast, the slow wave velocity, for those angles where it was observed, remains around 1500 m/s in both datasets. Discrepancies between the two sources of data for similar bone type and porosities may arise from the fact the Hosokawa samples had been saturated with water prior to testing, which is likely to affect measured velocities,<sup>16</sup> as well as differences in experimental method.

Figure 5(a) shows the predictions of the Stratified Biot and Schoenberg models calculated for the minimum and maximum porosity values of the samples tested, these being  $\beta=0.65$  and 0.82. This yielded a pair of curves for each wave predicted, such that a tested sample with a porosity within this range would yield a velocity within these bounds. This approach is preferable to comparing all data to one prediction with a single porosity value. Clearly, the effect of varying input porosity between these bounds (roughly a 20% change) has a greater effect on the Stratified Biot model, which displays a change in fast wave velocity of roughly 500 m/s (also 20%), than on the Schoenberg model, which, at its greatest, displays a change of less than 100 m/s (6%).

The performance of the Stratified Biot model is varied. First, the Stratified Biot model gives poorer agreement with slow wave data than the Schoenberg model, both quantitatively and in the curvature of its angular variation. Some discrepancy may arise because the omission of shear in the development of the stratified tortuosity reduces the slow wave velocity in Eq. (1) to zero, and thus only the expression for the Biot fast wave is equated with Eq. (8). This may reduce the influence of the slow wave in this approach. Nevertheless, at  $0^\circ$ , where the slow wave velocity is reduced to 0 m/s, the models are in agreement.

In the case of the fast wave, two differing outcomes are seen. First, between  $0^\circ$  and  $20^\circ$ , Schoenberg's theory continues to provide better agreement with the Hughes *et al.* data, although not with that of Hosokawa and Otani. However, the Stratified Biot model improves agreement with data over a larger angular range from  $30^\circ$  to  $90^\circ$ . This effect is illustrated more clearly in Fig. 5(b). Figure 5(b) shows fast wave data selected between  $30^\circ$  and  $90^\circ$  only, where the Stratified Biot model is evaluated for the porosity of each sample tested. Agreement is considered to have been improved in two areas. First, the Stratified Biot model enhances quantitative agreement to data with porosity, an effect not predicted by Schoenberg's theory to any similar degree. Second, the shallower curvature of the Stratified Biot model improves agreement over this wide angular range. This is particularly seen

in the case of the data from the sample with a porosity of 0.82, where the prediction is, to within 4%, inside the experimental error.

Hence, it may be concluded that the introduction of a stratified tortuosity within Biot's theory enhances the correlation with the current fast wave data at high propagation angles, although Schoenberg's model remains superior for low angles and the slow wave.

As an aside, these results may be further judged in the context of clinical utility. Many QUS systems test the calcaneus in the mediolateral axis, where the dominant trabecular microstructure may be assumed to be perpendicular to the direction of insonation, i.e., close to  $0^\circ$ . It is at low angles, however, where the Stratified Biot model does not perform as well as Schoenberg's theory. Thus, a limited attempt was made to improve agreement to fast wave data at low angles.

## VII. INTRODUCTION OF DIRECTIONAL INPUT PARAMETERS

While the Stratified Biot model introduces anisotropy through its description of the porous geometry, anisotropy also arises through mechanical properties of the cancellous matrix. Parameters such as the Young's modulus and Poisson's ratio of bone are dependent on direction;<sup>31</sup> indeed, highly anisotropic cancellous bone can display a ten fold difference in moduli depending on the loading direction with respect to trabecular orientation.<sup>1</sup> Much bone is also transversely isotropic, where properties are similar in a plane perpendicular to a longitudinal axis, and are significantly different from properties in the longitudinal direction.

Mechanical anisotropy was introduced into the Stratified Biot model in a simple empirical way. Gibson and Ashby<sup>1</sup> reported the Young's modulus of human cortical bone along the longitudinal axes as 18.1–22.6 GPa, and perpendicular to this, as 10.2–11.5 GPa. Taking rounded averages for each axes, with  $90^\circ$  representing the trabecular direction in testing, an angle-dependent Young's modulus for an anisotropic medium may be expressed as

$$E_s(\theta) = E_s(0^\circ) \sin^2(\theta) + E_s(90^\circ) \cos^2(\theta), \quad (11)$$

where  $E_s(0^\circ) = 10$  GPa and  $E_s(90^\circ) = 20$  GPa.

The results of introducing  $E_s(\theta)$  into the Stratified Biot model can be seen in Fig. 6. Figure 6 shows predictions at the maximum and minimum porosities from both models, and data is as in previous figures.

The inclusion of  $E_s(\theta)$  provides no improvement in agreement with slow wave data, possibly because solid properties such as moduli are more associated with fast wave propagation. One significant shortcoming with the modification is that quantitative agreement at higher angles is somewhat degraded for some data. However, the fast wave predictions of the stratified Biot model and Schoenberg's theory become closer in shape, with the former being reduced by roughly 500 m/s at  $0^\circ$  and slightly flattening over  $10^\circ$ – $30^\circ$ . Furthermore, it should be noted that for individual samples, the consistent error in the Stratified Biot  $E_s(\theta)$  model of roughly 9% is comparable with the worst error in Schoenberg's model (of  $\sim 10\%$  against porosity-matched curves).

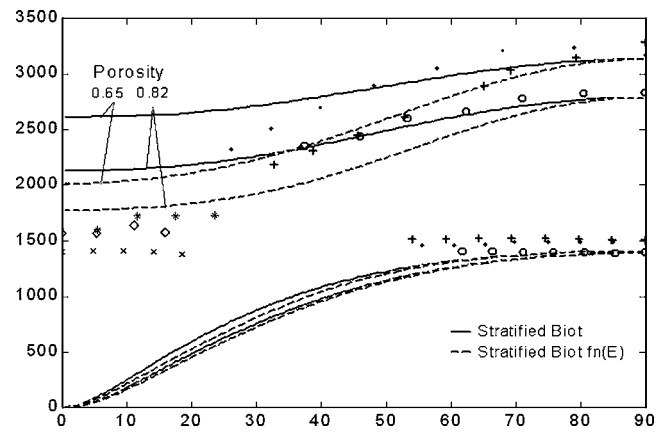


FIG. 6. Predicted and measured fast wave phase velocities versus propagation angle for the Stratified Biot model (solid line) and a stratified Biot model including directional Young's modulus (dashed line), evaluated at the upper and lower porosity limits. The angle  $0^\circ$  is normal to the structure [data from Hughes *et al.* (Ref. 6)].

Hence, although this approach would benefit from further study, the inclusion of angle-dependent mechanical properties such as  $E_s(\theta)$ , as well as structural ones such as  $\alpha(\theta)$ , appears to have some value in anisotropic propagation models.

## VIII. CONCLUSION

In this paper we have shown that the introduction of an angle-dependent tortuosity for a layered medium in a Biot model leads to the prediction of direction-dependent wave properties. Thus, the anisotropic response of ultrasound in cancellous bone may be partly attributed to the angular variation in inertial coupling.

While work on an anisotropic propagation model for cancellous bone requires further development, it has nonetheless been a key aim of this paper to highlight the fundamental importance of the tortuosity. Expressions for tortuosity may be easily manipulated and adapted to describe the varying architecture of cancellous bone. Where the use of tortuosity may be most valuable is in describing the deterioration of the cancellous structure, owing to the onset of osteoporosis. Changes such as the erosion of calcified plates and rods, and loss of anisotropy, cannot be completely described by the porosity or factors such as pore size, plate separation, or trabecular thickness. What remains to be investigated is whether an analysis of an adaptable tortuosity may give valuable information in the assessment of bone, whether *in vitro* or with clinical utility.

## ACKNOWLEDGMENTS

The authors would like to acknowledge the contribution of Professor Robert C Chivers, Visiting Professor at ISVR (1998–2001), who died in November 2004. Bob was a key advisor during the research, providing invaluable guidance drawn from his vast knowledge of physical acoustics. His groundbreaking research paved the way for our current understanding of ultrasonic propagation in biological tissue.

The authors also appreciate the collaboration of Dr. Kang II Lee, of ISVR and the Department of Physics and Institute of Basic Science, Sungkyunkwan University, Republic of Korea.

- <sup>1</sup>L. J. Gibson and M. Ashby, "Cancellous bone," in *Cellular Solids—Structure and Properties* (Pergamon, Oxford, 1998), Chap. 11, pp. 316–331.
- <sup>2</sup>C. F. Njeh, D. Hans, T. Fuerst, C.-C. Glüer, and H. K. Genant, "Basic sciences," in *Quantitative Ultrasound: Assessment of Osteoporosis and Bone Status* (Martin Dunitz Ltd, London, 1999), Chap. 1, pp. 1–101.
- <sup>3</sup>M. A. Biot, "Theory of propagation of elastic waves in a fluid saturated porous solid, II. High frequency range," *J. Acoust. Soc. Am.* **28**, 179–191 (1956).
- <sup>4</sup>M. L. McKelvie and S. B. Palmer, "The interaction of ultrasound with cancellous bone," *Phys. Med. Biol.* **36**, 1331–40 (1991).
- <sup>5</sup>J. L. Williams, "Ultrasonic wave propagation in cancellous and cortical bone: predictions of some experimental results by Biot's Theory," *J. Acoust. Soc. Am.* **92**, 1106–1112 (1992).
- <sup>6</sup>W. Lauriks, J. Thoen, I. Van Asbroek, G. Lowet, and G. Van der Perre, "Propagation of ultrasonic pulses through trabecular bone," *J. Phys. IV* **4**, 1255–1258 (1994).
- <sup>7</sup>J. L. Williams, M. J. Grimm, F. W. Wehrli, K. R. Foster, and H.-W. Chung, "Prediction of frequency and pore-size dependent attenuation of ultrasound in trabecular bone using Biot's Theory," in *Mechanics of Poroelastic Media* (Kluwer Academic, Netherlands, 1996), pp. 263–71.
- <sup>8</sup>A. Hosokawa and T. Otani, "Ultrasonic wave propagation in bovine cancellous bone," *J. Acoust. Soc. Am.* **101**, 558–562 (1997).
- <sup>9</sup>E. R. Hughes, T. G. Leighton, G. W. Petley, and P. R. White, "Ultrasonic propagation in cancellous bone: A new stratified model," *Ultrasound Med. Biol.* **25**, 811–821 (1999).
- <sup>10</sup>K. I. Lee, H.-S. Roh, and S. W. Yoon, "Acoustic wave propagation in bovine cancellous bone: Application of the Modified Biot-Attenborough model," *J. Acoust. Soc. Am.* **114**, 2284–2293 (2003).
- <sup>11</sup>Z. E. A. Fellah, J. Y. Chapelon, S. Berger, W. Lauriks, and C. Depollier, "Ultrasonic wave propagation in human cancellous bone: Application of Biot theory," *J. Acoust. Soc. Am.* **116**, 61–73 (2004).
- <sup>12</sup>K. A. Wear, A. Laib, A. P. Stuber, and J. C. Reynolds, "Comparison of measurements of phase velocity in human calcaneus to Biot theory," *J. Acoust. Soc. Am.* **117**, 3319–3324 (2005).
- <sup>13</sup>C.-C. Gluer, C. Y. Wu, and H. K. Genant, "Broadband ultrasound attenuation signals depend on trabecular orientation," *Osteoporosis Int.* **3**, 185–191 (1993).
- <sup>14</sup>P. H. F. Nicholson, M. J. Haddaway, and M. W. J. Davie, "The dependence of ultrasonic properties on orientation in human vertebrae," *Phys. Med. Biol.* **39**, 1013–24 (1994).
- <sup>15</sup>A. Hosokawa and T. Otani, "Acoustic anisotropy in bovine cancellous bone," *J. Acoust. Soc. Am.* **103**, 2718–2722 (1998).
- <sup>16</sup>P. H. F. Nicholson and M. L. Bouxsein, "Bone marrow influences quantitative ultrasound measurements in human cancellous bone," *Ultrasound Med. Biol.* **28**, 369–375 (2002).
- <sup>17</sup>E. R. Hughes, T. G. Leighton, G. W. Petley, P. R. White, and R. C. Chivers, "Estimation of critical and viscous frequencies for Biot theory in cancellous bone," *Ultrasonics* **41**, 365–368 (2003).
- <sup>18</sup>J. G. Berryman, "Confirmation of Biot's theory," *Appl. Phys. Lett.* **37**, 382–384 (1980).
- <sup>19</sup>C. Zwikker and C. W. Kosten, *Sound Absorbing Materials* (Elsevier, New York 1949), Chap. 8, p. 21.
- <sup>20</sup>D. L. Johnson, J. Koplik, and R. Dashen, "Theory of dynamic permeability and tortuosity in fluid-saturated porous media," *Fluid Dyn.* **176**, 379–402 (1987).
- <sup>21</sup>Z. E. A. Fellah, S. Berger, W. Lauriks, C. Depollier, C. Aristegui, and J.-Y. Chapelon, "Measuring the porosity and the tortuosity of porous materials via reflected waves at oblique incidence," *J. Acoust. Soc. Am.* **113**, 2424–2433 (2003).
- <sup>22</sup>K. Attenborough, H.-C. Shin, Q. Qin, M. Fagan, and C. M. Langton, "Measurement of tortuosity in stereolithographical bone replicas using audiofrequency pulses," *J. Acoust. Soc. Am.* **118**, 2779–2782 (2005).
- <sup>23</sup>R. Strelitzki, V. Paech, and P. H. F. Nicholson, "Measurement of airborne ultrasonic slow waves in calcaneal cancellous bone," *Med. Eng. Phys.* **21**, 215–233 (1999).
- <sup>24</sup>M. Schoenberg, "Wave propagation in alternating solid and fluid layers," *Wave Motion* **6**, 303–320 (1984).
- <sup>25</sup>F. Padilla and P. Laugier, "Phase and group velocities of fast and slow compressional waves in trabecular bone," *J. Acoust. Soc. Am.* **108**, 1949–1952 (2000).
- <sup>26</sup>K. A. Wear, "A stratified model to predict dispersion in trabecular bone," *IEEE Trans. Ultrason. Ferroelectr. Freq. Control* **48**, 1079–1083 (2001).
- <sup>27</sup>M. Kaczmarek, J. Kubik, and M. Pakula, "Short ultrasonic waves in cancellous bone," *Ultrasonics* **40**, 95–100 (2002).
- <sup>28</sup>M. A. Biot, "Generalized theory of acoustic propagation in porous dissipative media," *J. Acoust. Soc. Am.* **34**, 1254–1264 (1962).
- <sup>29</sup>M. D. Sharma and M. L. Gogna, "Wave propagation in anisotropic liquid-saturated porous solids," *J. Acoust. Soc. Am.* **90**, 1068–1073 (1991).
- <sup>30</sup>M. Schoenberg and P. N. Sen, "Properties of a periodically stratified acoustic half-space and its relation to a Biot fluid," *J. Acoust. Soc. Am.* **73**, 61–67 (1983).
- <sup>31</sup>F. A. Duck, "Elastic moduli of bone and teeth," in *Physical Properties of Tissue: A Comprehensive Reference Book* (Cambridge, University Press, Cambridge, 1990), Chap. 5, pp. 139–146.
- <sup>32</sup>J. R. Wu and F. Cubberly, "Measurement of velocity and attenuation of shear waves in bovine compact bone using ultrasonic spectroscopy," *Ultrasound Med. Biol.* **23**, 129–34 (1997).